ELSEVIER

Biochimica et Biophysica Acta 1565 (2002) 6–16

BIOCHIMICA ET BIOPHYSICA ACTA
BBA

www.bba-direct.com

Use of peptide antibodies to probe for the mitoxantrone resistance-associated protein MXR/BCRP/ABCP/ABCG2

Thomas Litman [a], Ulla Jensen [a], Alastair Hansen [b], Kuang-Ming Covitz [c], Zhirong Zhan [c], Patricia Fetsch [c], Andrea Abati [c], Paul Robert Hansen [d], Thomas Horn [b], Torben Skovsgaard [a], Susan E. Bates [c,*]

[a] *Laboratory of Oncology, Herlev University Hospital, DK-2730 Herlev, Denmark*
[b] *Department of Pathology, Herlev University Hospital, DK-2730 Herlev, Denmark*
[c] *National Cancer Institute—Cancer Therapeutics Branch and Laboratory of Pathology, National Institutes of Health, Building 10, Room 12N226, 9000 Rockville Pike, Bethesda, MD 20892, USA*
[d] *Department of Chemistry, Royal Veterinary and Agricultural University, DK-1871 Copenhagen, Denmark*

Received 18 March 2002; received in revised form 13 June 2002; accepted 13 June 2002

Abstract

Recent studies have characterized the ABC half-transporter associated with mitoxantrone resistance in human cancer cell lines. Encoded by the *ABCG2* gene, overexpression confers resistance to camptothecins, as well as to mitoxantrone. We developed four polyclonal antibodies against peptides corresponding to four different epitopes on the mitoxantrone resistance-associated protein, ABCG2. Three epitopes localized on the cytoplasmic region of ABCG2 gave rise to high-affinity antibodies, which were demonstrated to be specific for ABCG2. Western blot analysis of cells with high levels of ABCG2 showed a single major band of the expected 72-kDa molecular size of ABCG2 under denaturing conditions. Immunoblot analysis performed under non-reducing conditions and after treatment with cross-linking reagents demonstrated a molecular weight shift from 72 kDa to several bands of 180 kDa and higher molecular weight, suggesting detection of dimerization products of ABCG2. Evidence of *N*-linked glycosylation was also obtained using tunicamycin and *N*-glycosidase F. Finally, both by light, fluorescence and electron microscopic immunohistochemical staining, we demonstrate cytoplasmic and predominantly plasma membrane localization of ABCG2 in cell lines with high levels of expression. Plasma membrane staining was observed on the surface of the chorionic villi in placenta. These results support the hypothesis that ABCG2 is an ABC half-transporter that forms dimers in the plasma membrane, functioning as an ATP-dependent outward pump for substrate transport.

Keywords: Polyclonal antibody; Western blot; Immunohistochemistry; Atypical multidrug resistance; MXR/BCRP/ABCP/ABCG2; ABC half-transporter

1. Introduction

A new drug resistance gene, which confers high levels of resistance to mitoxantrone, anthracyclines, and several camptothecins, has been identified as an ABC half-transporter. Reported from several laboratories, it was termed MXR, for mitoxantrone resistance gene, in our hands [1]; BCRP, for breast cancer resistance protein, by Doyle et al. [2]; and ABCP, for ABC transporter expressed in placenta, by Allikmets et al. [3]. Overexpression of this transporter leads to reduced accumulation of its substrates, which include mitoxantrone, anthracyclines, several camptothecins, rhodamine 123, prazosin, and Lysotracker Green [4,5]. The human gene nomenclature committee (HUGO) has recommended that this gene be identified as *ABCG2* [6]. The mouse orthologue for *ABCG2*, *Abcg2* (*abcp1*), is overexpressed in drug-resistant cell lines in which the orthologues for *MDR*-1 and *MRP* are deleted [7]. Overexpression of *Abcg2* (*abcp1*) resulted whether the selecting agent was topotecan, adriamycin, or mitoxantrone. Recently, it was determined that a mutation at amino acid 482, in the third transmembrane domain, conferred some of the disparate substrate specificity observed in drug-resistant cells [8]. An arginine is encoded at amino acid position 482 in cells containing wild-type ABCG2, conferring a narrower substrate specificity with resistance primarily to mitoxantrone

* Corresponding author. Tel.: +1-301-402-1357; fax: +1-301-402-1608.
E-mail address: sebates@helix.nih.gov (S.E. Bates).

0005-2736/02/$ - see front matter
PII: S0005-2736(02)00492-3

and the camptothecins. A threonine or glycine encoded at amino acid 482 results in a gain of function with the anthracyclines and rhodamine 123 added as substrates.

The *ABCG2* gene encodes a 655-amino-acid transmembrane protein, with a domain organization characteristic of ABC half-transporters [9]. These proteins typically contain six transmembrane segments and one ATP binding domain, and require dimerization with a partner protein to become functional transporters [10]. Half-transporters are in general localized to intracellular compartments, such as the endoplasmatic reticulum for TAP1/TAP2 [11,12]; peroxisomes for the ALD subfamily [13]; and the mitochondria for M-ABC1 and ABC7 [14,15]. The "full-size" ABC transporters, on the other hand, among which are P-glycoprotein and MRP, are typically situated in the plasma membrane, and are about twice the size of half-transporters, with 12–17 membrane spanning segments and two ATP binding sites [10].

Studies to date suggest that ABCG2 is a potent, new mechanism for conferring multiple drug resistance. To better characterize the protein, to define and localize the functional transport unit, and to define its role in clinical oncology, we undertook to develop and characterize a panel of polyclonal antibodies against several epitopes on ABCG2.

2. Materials and methods

2.1. Cell culture

All cell lines were grown in IMEM supplemented with glutamine (2 mM), fetal calf serum (10%), penicillin (100 u/ml), and streptomycin (100 μg/ml). Drug-resistant cells were maintained in the presence of the selecting drugs. The S1-M1-80 cells were generated in our lab by exposing the S1-M1-3.2 colon carcinoma cell line (established by Rabindran et al. [16]) to increasing concentrations of mitoxantrone. The S1-M1-80 cell line was maintained in 80 μM mitoxantrone [1]. The MCF-7-resistant sublines were derived by stepwise selection from parental MCF-7 breast carcinoma cells. The MCF-7 AdVp3000 cells were selected from MCF-7 parental cells and were cultured in 5.5 μM adriamycin plus 5.5 μM verapamil [17]. The MCF-7 FLV1000 cell line was selected in 1 μM flavopiridol as described by Robey et al. [18]. The MCF-7 MX cell line was obtained from Young et al. [19] and independently selected and cultured in mitoxantrone at 600 ng/ml.

2.2. Peptide synthesis

Peptide synthesis was accomplished manually using a stepwise Fmoc/t-Bu solid-phase peptide synthesis procedure [20] on TentaGel S RAM resin (Rapp Polymers, Tübingen, Germany). Following peptide synthesis and workup, the product was characterized by liquid-chromatography mass spectrometry. The peptide sequences and predicted localization within ABCG2 are indicated in Fig. 1.

2.3. Antibody production

Antibodies were obtained by immunizing New Zealand White rabbits with KLH-conjugated peptide (100 μg peptide per injection). Pre-immune bleeds were taken from all rabbits before the first injection. After immunization, bleeds were drawn from the ear vein at weeks 6, 8, and 10. The rabbits were boosted twice with the same peptide as used for the primary injection at 4-week intervals. We have named the antibodies after the rabbit identification number. The titer of each antibody was tested by an enzyme-linked immunosorbent assay (ELISA) using the immunizing peptide on the solid phase.

2.4. Cross-linking

Chemical cross-linking was performed in vivo on intact cells. After incubation at room temperature for 30 min with the cross-linking agents disuccinimidylsuberate (DSS) or dithiobis[succinimidylpropionate] (DSP) at 2 mM final concentration, the reaction was terminated by addition of Tris–HCl (pH 8) to 20 mM [14], and the cells were lysed. In enzymatic cross-linking experiments, ABCG2 containing microsomes were treated with tissue transglutaminase at 20 μg/ml at 37 °C for 30 min, before electrophoretic analysis [21].

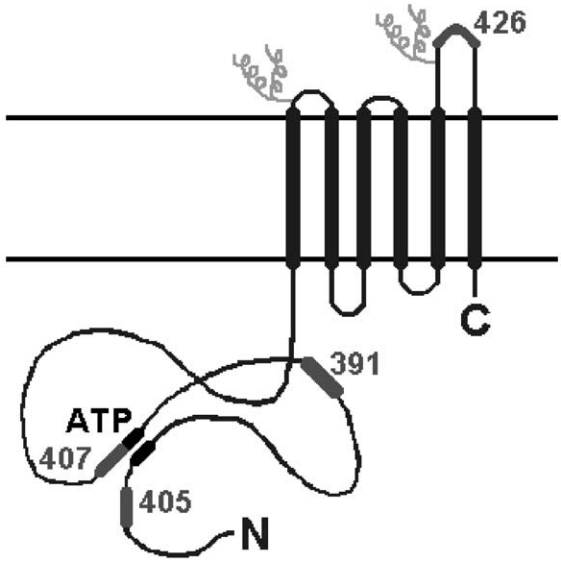

Fig. 1. Predicted secondary structure of ABCG2. The cartoon shows the positions of the four epitopes chosen for antibody production within the sequence of ABCG2. Also indicated is the ATP binding site (the Walker A and B motifs) and the putative *N*-glycosylation sites. The peptide sequences are: 405 (56–70): RKPVEKEILSNINGI; 391 (150–167): TTMTNHEKNERINRVIEE; 407 (208–221): SLDEPTTGLDSSTA; 426 (608–622): CTGEEYLVKQGIDLS.

2.5. Glycosylation analysis

To assess the level of glycosylation, two complementary methods were employed:

1) Enzymatic deglycosylation of ABCG2-containing microsomes with 2 I.U. *N*-glycosidase F was performed at 37 °C for 12 h [14], or
2) Cells were grown in the absence or presence of tunicamycin, which inhibits de novo *N*-linked glycosylation, at 5 μg/ml for 3 days [22].

2.6. Western blot analysis of proteins

Microsomal membranes (50 μg of protein) were incubated in SDS loading buffer (2% SDS, 10% glycerol, 1% beta-mercaptoethanol, 5 ppm bromophenol blue, 125 mM MOPS, pH 6.8) for 20 min without boiling. For experiments under non-reducing conditions, beta-mercaptoethanol was omitted from the loading buffer. The extracts were loaded onto an 8% (w/v) SDS–polyacrylamide gel and subjected to electrophoresis [23]. After electro-transfer onto nitrocellulose membranes (Bio-Rad, Hercules, CA), the blots were blocked with Tris-buffered saline containing 0.05% (v/v) Tween-20 and 5% (w/v) non-fat dry milk. Probing was performed overnight at 4 °C with the polyclonal anti-ABCG2 antibodies (in dilutions 1:500–1:3000), which were raised against 14–18-mer peptide fragments of ABCG2. After washing the membranes four times in TST (10 mM Tris–HCl, 150 mM NaCl, 0.05% Tween-20, pH 7.5), a secondary horseradish peroxidase-conjugated donkey anti-rabbit antibody (Affinity Bioreagents, Golden, CO) was applied for 1 h (dilution 1:2000) followed by enhanced chemiluminescence detection (NEN, Boston MA) with exposure on Kodak X-OMAT AR autoradiography film to visualize immunoreactive bands.

2.7. Immunoprecipitation

For immunoprecipitation, microsomal membranes were solubilized in RIPA buffer (150 mM NaCl, 1% Triton X-100, 0.1% SDS, 50 mM Tris–HCl, protease inhibitors: pepstatin A 10 μg/ml, leupeptin 10 μg/ml, aprotinin 5 μg/ml, PMSF 2 mM) for 30 min at 4 °C. Affinity-purified rabbit-anti-ABCG2 antibody 405 (75 μl) was cross-linked to a protein A column (total volume: 0.4 ml) with 5 mM DSS (Seize™ Protein A Immunoprecipitation Kit, Pierce, Rockford, IL). The soluble fraction from the RIPA extract was applied on the column and incubated overnight at 4 °C, end-over-end. Elution of the immune complexes was performed according to the protocol (Pierce). The eluted material was separated on a 7% NuPAGE tris-acetate gel (NOVEX, San Diego, CA), and silver stained, following the manufacturer's protocol (Pharmacia Biotech Silver staining kit, Pharmacia, Uppsala, Sweden).

2.8. Immunohistochemistry

Formalin-fixed paraffin embedded tissue blocks were cut into 5-μm sections. The sections were baked at 60 °C, deparaffinized in xylene and ethanol, microwaved for 5 min until boiling in Citra Plus (BioGenex), and then microwaved for another 15 min at low power. Tissue sections were quenched in 3% H_2O_2, and subsequently incubated in 5% goat serum for 20 min. An avidin–biotin block (Vector Laboratories, Burlingame, CA) was incorporated. Anti-ABCG2 polyclonal antibody (405, dilution 1:2500) was added to the section, and the slides were incubated for 2 h at room temperature. A biotinylated secondary antibody (goat anti-rabbit) was applied and slides were incubated for 30 min at room temperature. An avidin–biotin–peroxidase complex was formed and slides were incubated a further 30 min. Subsequently, 3,3′ -diaminobenzidene (DAB, Sigma, St. Louis, MO) was used to detect the bound peroxidase. On all samples, a negative sample control (rabbit immunoglobulins, DAKO, Carpinteria, CA) was also performed, and a positive control cell line (MCF7 MX100) was used throughout.

2.9. Immunofluorescence confocal microscopy

Cells (10^5/ml) were grown in phenol-red free IMEM for 48 h in eight-well glass chamberslides (Nunc, Roskilde, Denmark) before washing with PBS. After fixation in 1:1 methanol/ethanol for 1 min at room temperature, the slides were washed 10 min in PBS, and this washing step was repeated three times. Then the slides were incubated with 2% human AB serum (Sigma) for 2 h at room temperature and gentle shaking. Probing with the polyclonal antibody 405 at dilutions 1:3000–1:6000 was performed at 4 °C overnight. After washing four times 10 min with PBS, the secondary antibody, FITC-labeled pig-anti rabbit (DAKO, Denmark), was added for 1 h at a 1:100 dilution. A Zeiss LSM 410 confocal laser scanning microscope equipped with a 150-mW Omnichrome Ar–Kr laser exciting at 488 nm was used for excitation of the fluorescein label, and the emitted light passed through a 515- to 540-nm band-pass filter. Images were stored online to a ZIP disk (Iomega) and analyzed off-line in Paint Shop Pro v. 6.02 (Jasc, Eden Prairie, MN).

2.10. Immuno-electron microscopy

Cells were plated in 10 cm Petri dishes and grown in phenol-red free IMEM medium for 48 h before the medium was removed by aspiration. Then, the cells were washed with 0.1 M ice-cold phosphate buffer (PBS) and scraped from the surface of the culture flask. The cell suspension was washed once with PBS, centrifuged, fixed for 1 h with 4% (w/v) paraformaldehyde in 0.1 M PBS, and then washed again with PBS. The cell pellet was embedded in 15% (w/v) gelatin (Sigma, G-9382) in 0.1 M PBS at 37 °C for 10 min,

and then centrifuged at 4000 rpm for 5 min. After the gelatin solidified, it was cut into small pieces which were infiltrated with poly-vinyl-pyrolidone (PVP)-sucrose, and then frozen in liquid nitrogen [24]. Ultrathin sections were cut on a Leica EMFCS.

For immunostaining, the rabbit polyclonal antisera 405 and 391 were diluted 1:10,000 (after initial titration experiments with different antibody dilutions), goat anti-rabbit IgG conjugated to 1 nm colloidal gold particles (Aurion, Wageningen, The Netherlands) was diluted 1:300, and

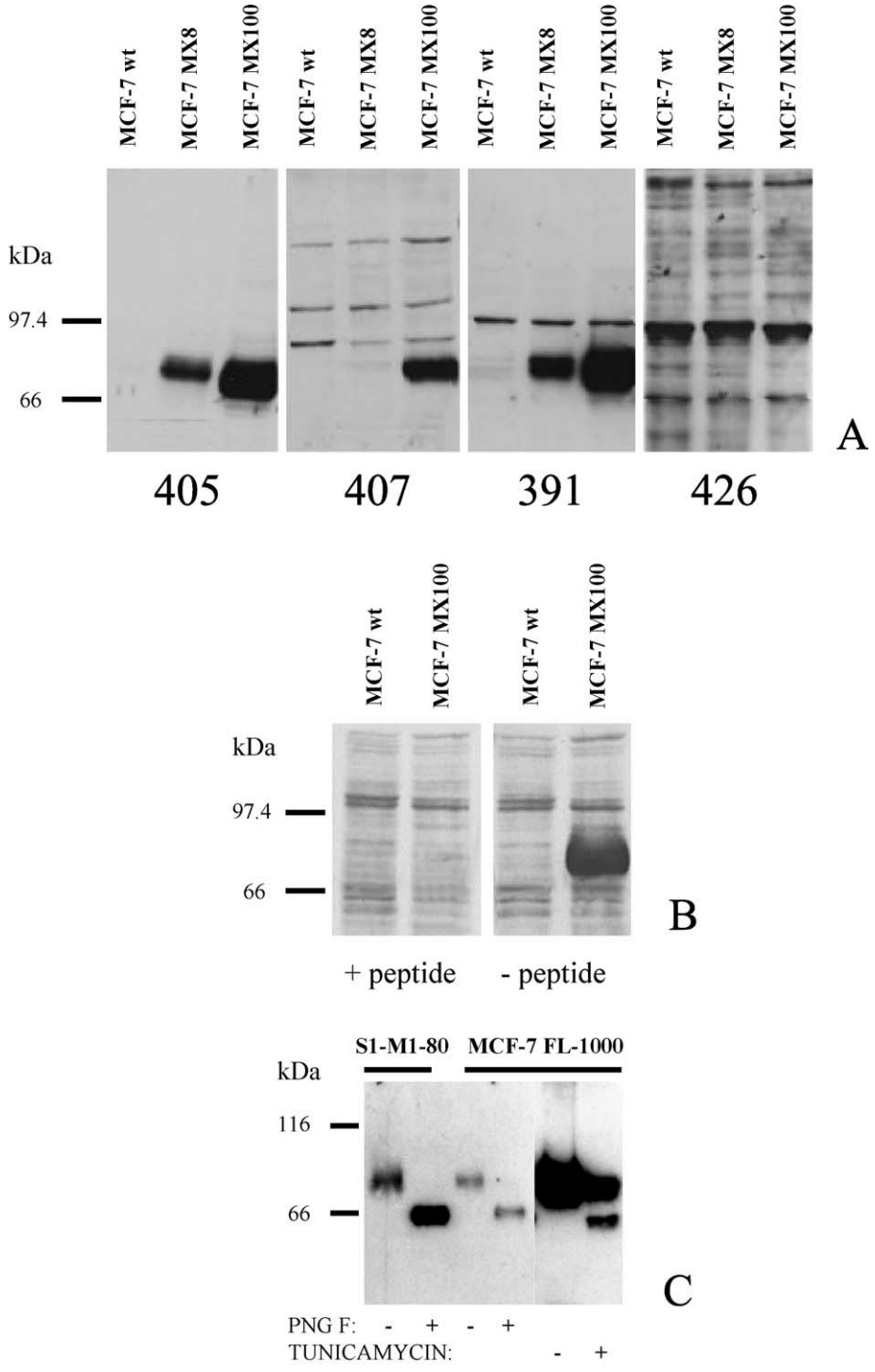

Fig. 2. Immunoblot screening of the four anti-sera 405, 407, 391, 426. (A) Antisera in ABCG2-overexpressing cell lines. (B) Anti-serum 405, which has or has not been preadsorbed with the peptide fragment used for immunization. (C) Glycosylation analysis: Treatment with either PNG F (*N*-glycosidase F) or tunicamycin reduces the apparent molecular weight of ABCG2 to its non-glycosylated form.

Protein A 5 nm particles (BioCell, Cardiff, England) were applied at a 1:75 dilution. Sections were blocked by incubation in 20 mM glycine and 0.1% (w/v) skim milk powder in PBS for 15 min, followed by incubation with primary antibody overnight at 4 °C. After washing with 0.1% (w/v) skim milk in PBS for 20 min, the sections were incubated with goat anti-rabbit 1 nm gold/Protein A in 0.1% (w/v) skim milk/PBS containing 0.06% (v/v) polyethyleneglycol and 2.2% (w/v) fish gelatin for 2 h. Sections were washed with 0.1% (w/v) skim milk in PBS for 30 min, postfixed in 2% (w/v) glutaraldehyde and washed again with distilled water before silver enhancement (R-GENT, Aurion, Wageningen, The Netherlands) for 45 min. Finally, the sections were contrasted in uranyl acetate for 5 min followed by a 5-min incubation in acidic uranyl acetate/methyl cellulose [25]. Control experiments included pre-immune serum, primary antibody adsorbed to the immunizing peptide, as well as omitting the primary antibody. Sections were viewed in a Philips 208 transmission electron microscope.

3. Results

3.1. Antibody production

From the predicted secondary structure of ABCG2, BLAST [26] searches, and antigenicity plots (not shown), we chose four different epitopes on ABCG2 for peptide synthesis and antibody production. The epitopes are indicated in Fig. 1 and correspond to a region just before the N-terminal Walker A motif (56–70: RKPVEKEILSNINGI), an area between the Walker A and B domain (150–167: TTMTNHEKNERINRVIEE), a peptide including the Walker B site (208–221: SLDEPTTGLDSSTA), and an amino acid stretch which is part of a large extracellular loop (608–622: CTGEEYLVKQGIDLS) close to the C-terminal. A BLAST search of the GenBank protein database indicates that all four of the peptides have 100% identity only with ABCG2. The sequence near the Walker A motif (56–70: RKPVEKEILSNINGI) and the sequence between Walker A and B (150–167: TTMTNHEKNERINRVIEE), are so distinct that even allowing four mismatches, the only hits retrieved were the same gene, AF098951 (BCRP) and AF103796 (ABCP1).

3.2. Immunoblot analysis

Results of immunoblot analysis with the panel of four antisera are shown in Fig. 2A: 405 (peptides 56–70); 391 (peptides 150–167); and 407 (peptides 208–221). The fourth antiserum, 426 (peptides 608–622) failed to generate a specific signal, and results obtained with this antibody are not shown in subsequent experiments. The 405, 407, and 391 antibodies all detect a 72-kDa band in membrane extracts from ABCG2 overexpressing (by Northern blot) cells: MCF-7 MX8 (intermediate ABCG2 expression), and MCF-7 MX100 (high ABCG2 expression). The 72-kDa band found corresponds well to the predicted molecular weight of ABCG2. No bands were detected in control lanes with microsomal membranes from cells with very low levels of ABCG2 expression, MCF-7 wt, as measured by Northern blot. Specificity of the antibodies was further confirmed using pre-immune serum (data not shown) and anti-serum preadsorbed with the immunizing peptide for 1 h at 37 °C. Only the result with the 405 preadsorbed antibody is shown in Fig. 2B; results with the other two specific antibodies were comparable. The 405 antibody, raised against a peptide corresponding to the region 5′ to

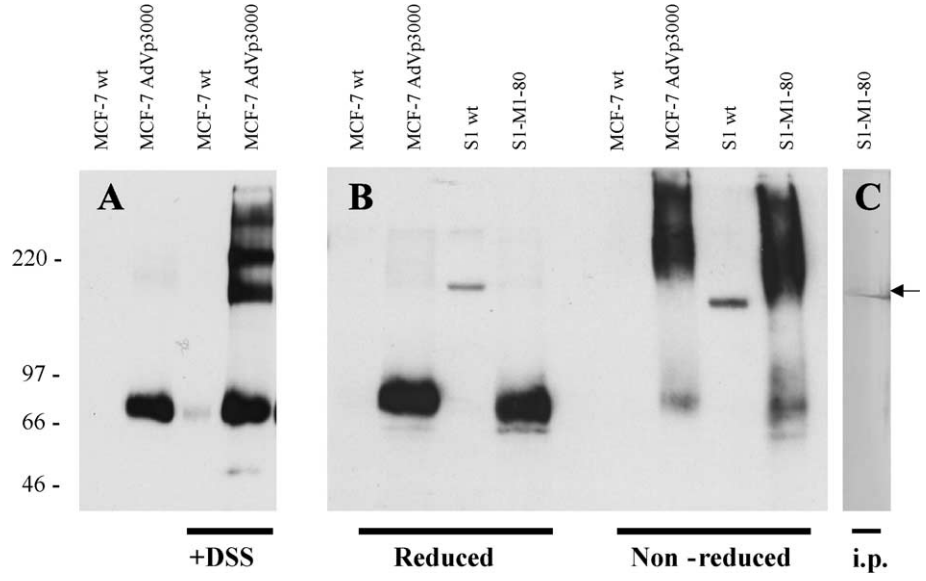

Fig. 3. Apparent dimerization of ABCG2. (A) Chemical cross-linking with DSS, (B) the effect of reduced vs. non-reduced SDS-PAGE conditions, and (C) silver-stained gel after immuno-precipitation of S1-M1-80 membranes.

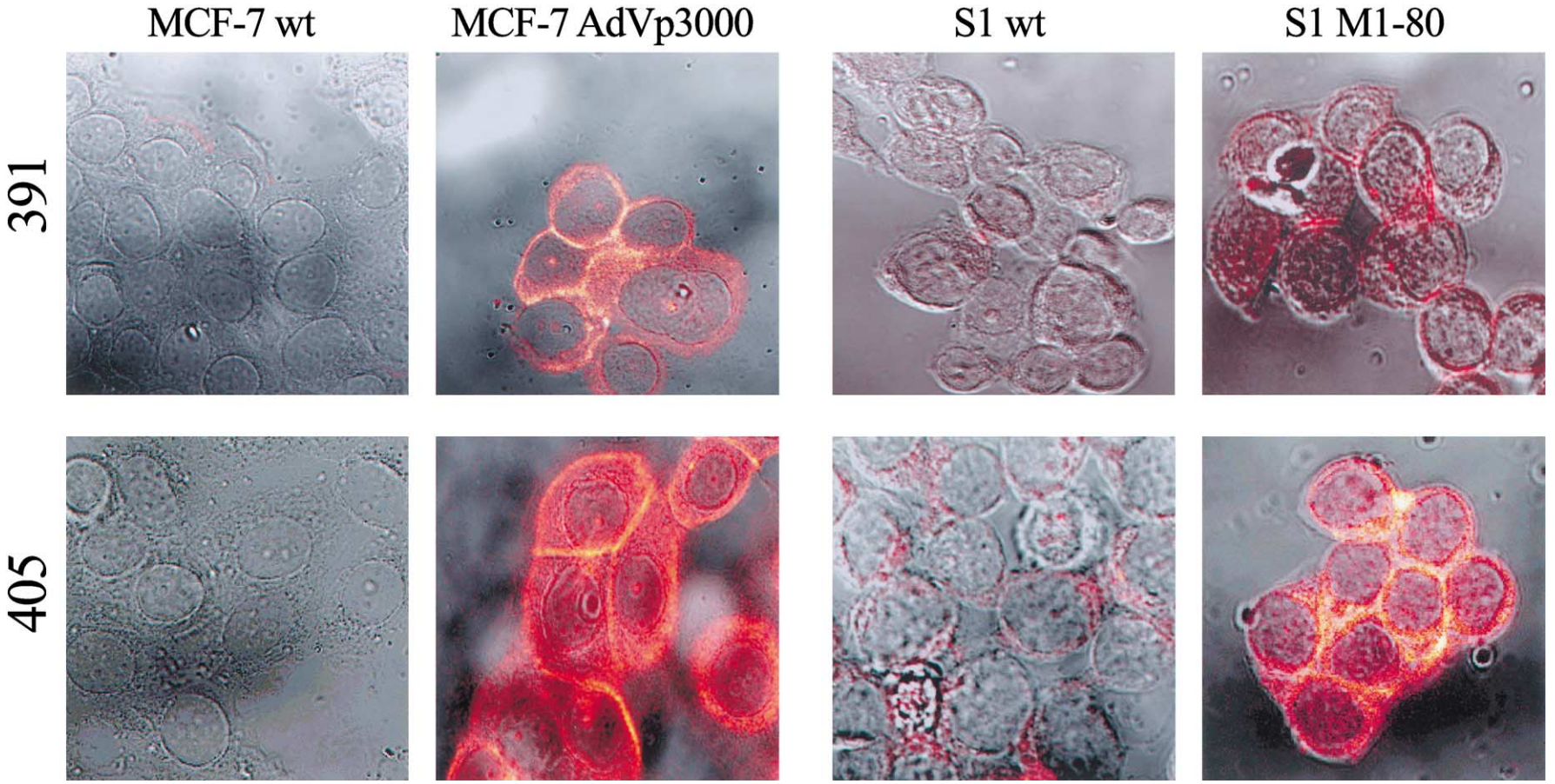

Fig. 4. Confocal microscopic images of immunofluorescence assay using the two anti-sera 391 and 405 on S1 and MCF-7 parental cells and on ABCG2-positive MCF-7 AdVp3000 and S1-M1-80 cells. ABCG2 localization to the plasma membrane is observed also with MCF-7 MX8, MCF-7 MX100, and MCF-7 FLV1000 cells (data not shown).

the Walker A site, gave a higher level of signal than the other antisera.

To assess whether ABCG2 was post-translationally modified by addition of oligosaccharide at one or both of its potential *N*-linked glycosylation sites, immunoblotting was performed on microsomes treated with *N*-glycosidase F, and on cells grown in the presence of tunicamycin, which inhibits *N*-glycosylation. As shown in Fig. 2C, both treatments lead to a significant reduction in the apparent molecular mass of ABCG2, suggesting that ABCG2 does contain *N*-linked oligosaccharide, probably at both the putative glycosylation sites.

3.3. Detection of dimerization products

The chemical cross-linkers DSP and DSS were used to link proteins in close proximity, 12 and 11.4 Å, respectively. Both reagents induced formation of high-molecular-weight products, which were detected by the anti-ABCG2 405 antibody. Three bands, with molecular weight 180 kDa or greater, were identified in cell lysates from MCF-7 AdVp3000, but not the parental MCF-7 cells (Fig. 3A, only results with DSS are shown). The formation of these bands was dependent on the presence of the cross-linking agent, DSS. Interestingly, similar high-molecular-weight bands were also observed when the cell lysates were run in SDS-PAGE gels under non-reducing conditions (without DTT and beta-mercaptoethanol) as shown in Fig. 3B. These bands were not detected when the gel was run under reducing conditions. Identical results, that is, the appearance of a high-molecular-weight complex that disappeared after treatment with beta-mercaptoethanol, were obtained with enzymatic, transglutaminase-catalyzed cross-linking of ABCG2-containing S1-M1-80 membranes (data not shown). The high-molecular-weight bands suggest that ABCG2 may oligomerize with other proteins, and most likely, with itself. The latter notion is supported by the immunoprecipitation experiment depicted in Fig. 3C. Here, only a single MW ~ 140-kDa band, corresponding to a possible ABCG2 dimer, appears on the silver-stained gel after elution from the protein-A-antibody immunoprecipitation column.

3.4. Immunofluorescence confocal microscopy

Previous immunohistochemical studies in the selected cell lines using the 405 antibody suggested a plasma membrane localization for ABCG2 [4,27]. We asked whether similar results would be obtained with an immunofluorescence technique using sensitive confocal microscopy.

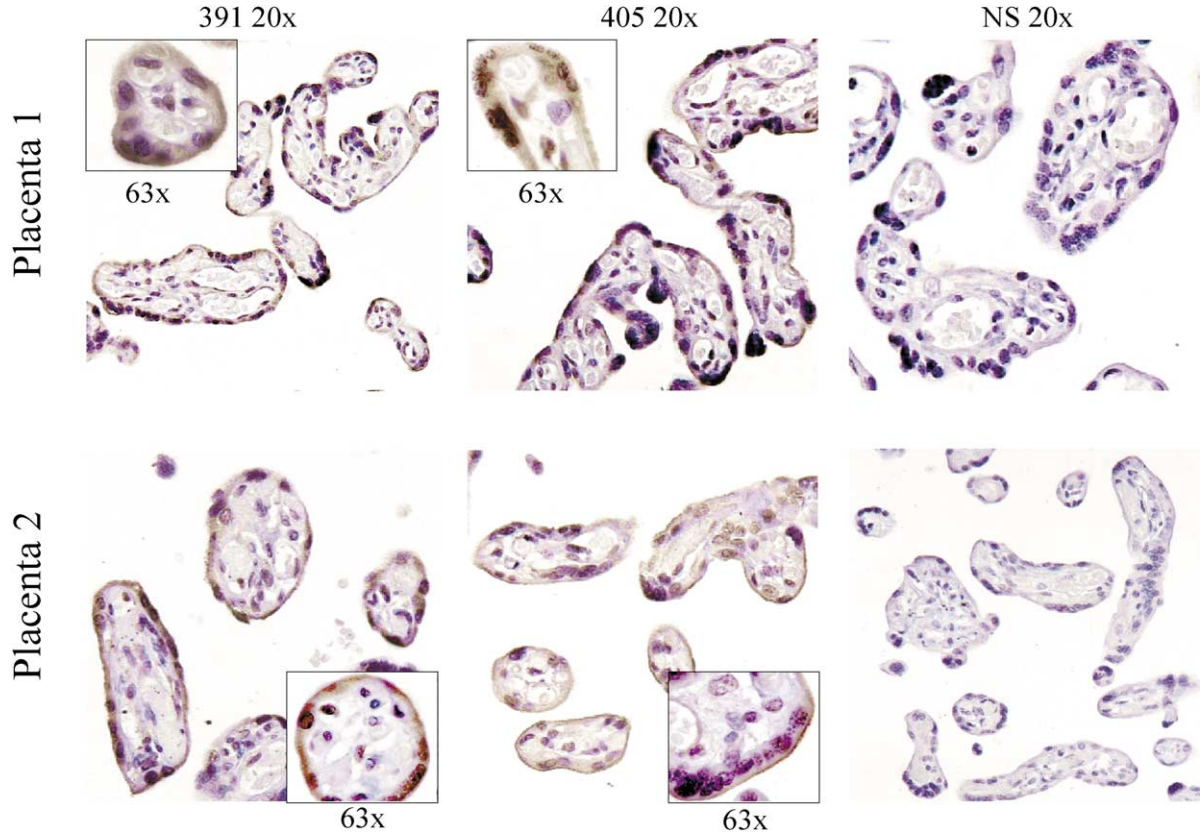

Fig. 5. Immunohistochemistry on paraffin sections of two mid-term, normal placentas. The staining was performed as described in Materials and Methods. Antibodies 391 and 405 at 1:3000 dilution were applied as well as control staining with non-immune serum (NS). Note staining on the cell surface of the synchitiotrophoblast cell layer of the chorionic villi.

Fig. 4 displays the membrane and intracellular localization of ABCG2 in S1-M1-80 and MCF-7 AdVp3000 cell lines by confocal microscopy using immunofluorescence. Similar localization of ABCG2 was observed with MCF-7 FLV1000 and MCF-7 MX cells. Only background levels of ABCG2 were detected in the parental cell lines, S1 wt and MCF-7

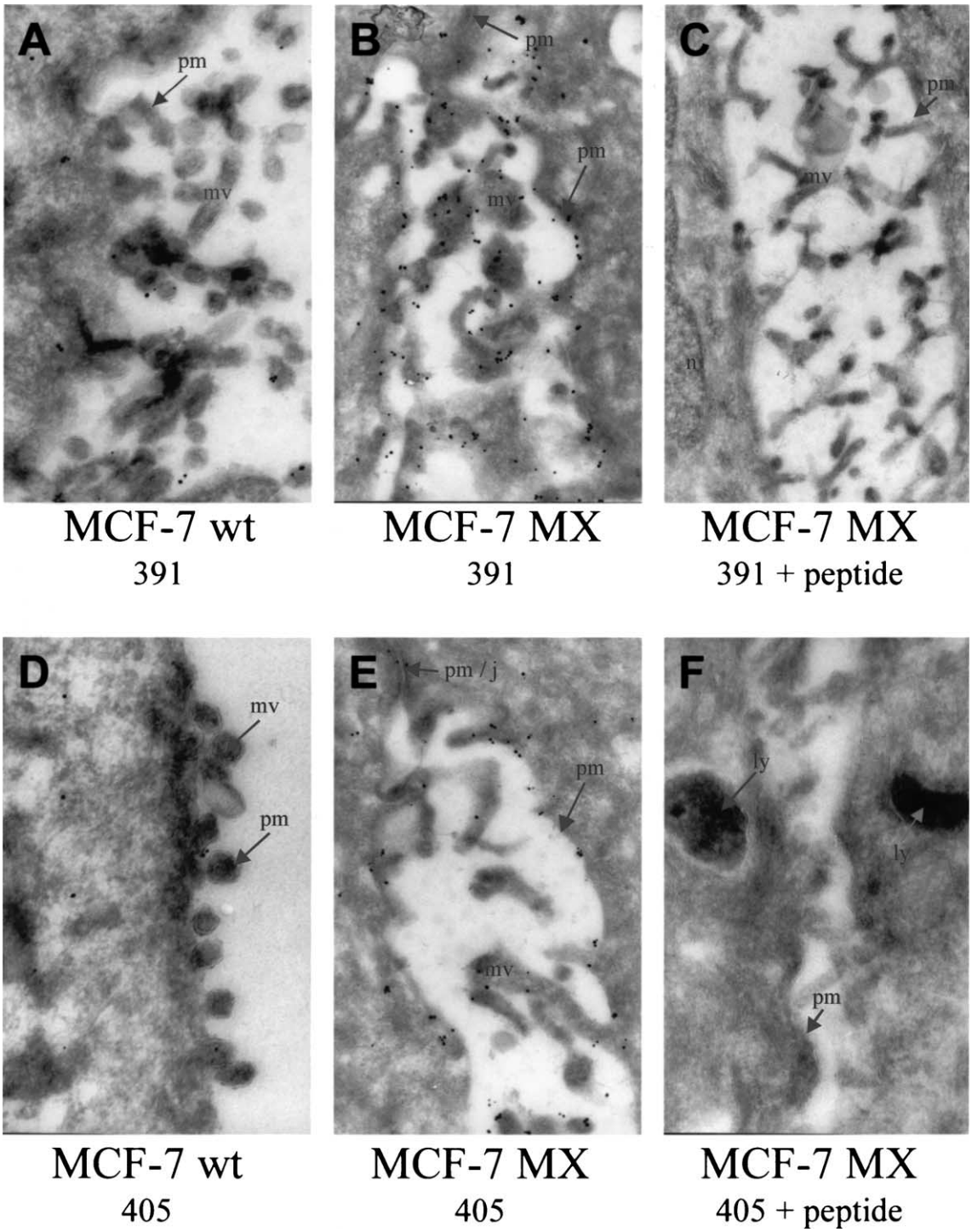

Fig. 6. Immuno-electron microscopy with 1 nm immunogold. The top panels (A,B,C) have been stained with anti-ABCG2 antibody 391, and the lower panels (D,E,F) with the anti-ABCG2 antibody 405. Wild-type cells stained consistently negative (A,D), while drug-resistant MCF-7 MX cells showed labeling of the cell membrane (B,E). This specific membrane labeling was eliminated by blocking with the antibody-specific peptide (C,F). Magnification × 16,000 in all panels. Abbreviations: pm, plasma membrane; mv, microvillus (microvilli); n, nucleus; j, junction; ly, lysosome. Panels A and D show part of the cell surface of one cell, while B, C, E and F show microvilli-containing opposing surfaces of two cells. The big dense blobs on A are chromagen deposits (staining artifacts) that can be observed in cells in which antibody has not been added.

wt. Control experiments with primary antibody preadsorbed with the peptide used for immunization, as well as incubation with pre-immune serum only, showed no specific labeling (data not shown).

3.5. Immunohistochemistry

Before studies aimed at determination of the normal tissue expression pattern, we evaluated the ability of the antibodies to detect ABCG2 in tissues fixed in paraffin. Since high levels of expression were observed by Northern blot in placenta [3], we used that tissue to assess the ability of these antibodies to detect ABCG2 in paraffin-embedded samples. As shown in Fig. 5, membrane staining is noted on the surface of synchitiotrophoblastic cells of the chorionic villi. The 405 antibody, as in the immunoblot analysis, gave a stronger signal than the 391 antibody. Plasma membrane staining was seen with both antibodies, as shown in the insets. Peptide competition studies demonstrated loss of specific antibody staining (data not shown), and non-immune serum (NS) showed consistent negative staining.

3.6. Immuno-electron microscopy

Ultrathin cryosections of MCF-7 cells were stained with 1 nm immunogold for the evaluation of ABCG2 antigen expression using both anti-ABCG2 antibodies 391 and 405. Wild-type MCF-7 cells stained consistently negative (Fig. 6A,D), while mitoxantrone-resistant MCF-7 MX cells displayed a distinct labeling on the cell surface membrane (Fig. 6B,E). This membrane staining was eliminated by adsorption of the antibody to the corresponding peptide used for immunization (Fig. 6C,F). Membrane staining was also observed on intracellular luminae containing slender, microvillus-like cell projections (data not shown). In drug-resistant MCF-7 MX cells, cytoplasmic labeling was seen inside empty-looking vesicles (Fig. 7). The nature of these vesicles remains unknown since they did not show any resemblance to lysosomes, Golgi saccules, mitochondria or endoplasmic reticulum (ER). The latter structures are all stained negatively. No major differences in staining pattern or intensity could be detected between the two antibodies (Fig. 6) or between crude serum preparations and affinity-purified antibody fractions (data not shown).

In an attempt to evaluate a possible di- or polymerization of the ABCG2 protein molecules, anti-ABCG2 antibodies were labeled with protein A to achieve a 1:1 grain/antigen ratio. Protein A tagging appeared as separate grains in all positively stained areas (data not shown). Similar results were obtained with MCF-7 AdVp3000 cells, though the labeling was less concentrated than what was observed with MCF-7 MX cells. The latter cells appear to have the highest expression level of ABCG2 of all cell lines so far tested. Labeling of S1-M1-80 cells was close to background levels

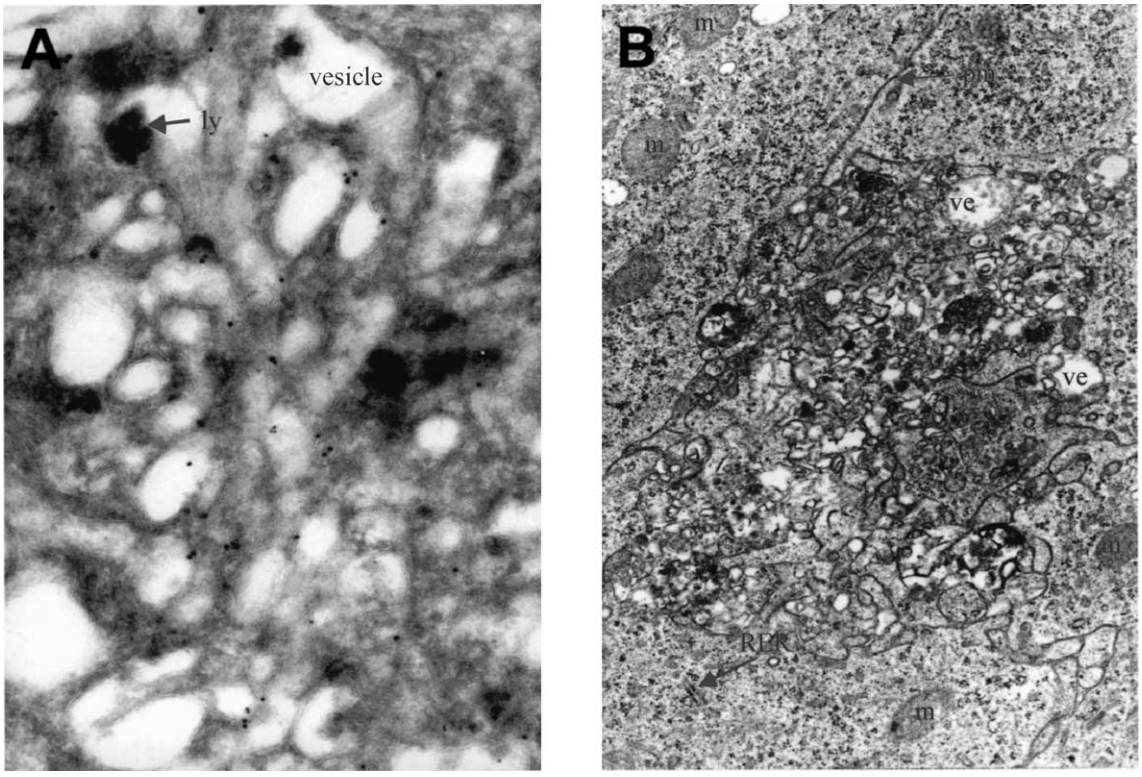

Fig. 7. (A) Immuno-electron microscopy with antibody 405 and 1 nm immunogold. Magnification ×16,000. (B) Conventional electron microscopy for morphological resolution. Magnification ×6,300. ABCG2 antigen expression is seen in cytoplasmic empty-looking vesicles that do not resemble lysosomes, Golgi saccules, mitochondria or ER. Abbreviations: pm, plasma membrane; ly, lysosome microvillus (microvilli); n, nucleus; j, junction; ly, lysosome.

suggesting that only high levels of ABCG2 will be detected by the immuno-electron microscopy.

4. Discussion

To aid in evaluating the mechanism of action and function of the ABC half-transporter ABCG2 and to facilitate its detection in clinical trials, we generated a series of rabbit polyclonal antibodies. These antibodies were produced against four predicted peptide epitopes on the ABCG2 protein. Three of these antibodies, derived from peptides predicted to be in the cytoplasmic region, proved to be of high affinity, while no specific binding could be detected with the fourth antibody. The antibodies confirmed the expected 72-kDa molecular size of ABCG2. The protein was shown to be highly glycosylated, probably on both the putative *N*-glycosylation sites, and enzymatic deglycosylation decreased the molecular weight to that found with ABCG2 expressing Sf9 cells [22]. Cross-linking studies and electrophoresis under non-reducing conditions suggest that ABCG2 undergoes dimerization or higher orders of oligomerization. Both cytoplasmic and plasma membrane localization were observed by confocal microscopy, by immunohistochemistry and by immuno-electron microscopy in drug-selected cell lines with high levels of ABCG2 expression, while no staining was detectable on the cell surface of parental cells.

The ABC half-transporter MXR (ABCG2) was identified in human colon carcinoma cells highly resistant to mitoxantrone. This protein is identical to the breast cancer resistance associated protein (BCRP), and to the placenta-specific ABC transporter (ABCP1) [2,3]. The substrate specificity has been the subject of several studies, which in accordance have demonstrated high levels of mitoxantrone resistance, with cross-resistance to certain camptothecins including topotecan and SN-38 [5,7,28]. Mutation at amino acid 482 results in a gain of function that produces an increase in the overlap in substrate specificity with P-glycoprotein. Yet, there is a lack of sensitivity to most inhibitors of P-glycoprotein. As such, ABCG2 is a potential candidate to explain some of the failures of P-glycoprotein antagonists to improve therapeutic outcome in clinical trials [29].

The peptides chosen for the antisera corresponded to four 14- to18-mer peptide sequences on ABCG2–3 cytoplasmic regions near the ATP binding domain and one region corresponding to a putative extracellular loop. The antibody 405 was generated to sequence RKPVEKEILSNINGI, peptides 56–70, 5′ to the Walker A sequence. The antibody 391 was generated to sequence TTMTNHKNERINRVIEE, peptides 150–167, near the C signature region. The antibody 407 was generated to sequence SLDEPTTGLDSSTA, peptides 208–221, including the Walker B site.

One of the most intriguing questions involving ABCG2 is its localization. The three previously known subfamilies of human half-transporters have intracellular localization. The TAP1 and 2 genes localize to the ER for their role in the transport of antigen into the ER for loading onto the major histocompatibility complex type I (MHCI) [12]. The peroxisomal transporters ALDP, PMP 70, and PMP 69R localize to the peroxisome for their role in the transport of lipids for beta-oxidation [30]. M-ABC1 and ABC7 have a mitochondrial localization [14,15]. Thus, it could be expected that ABCG2 would localize to an intracellular organelle. However, the 405 antibody has demonstrated plasma membrane staining by both confocal microscopy and by immunohistochemistry [4,27]. These findings are similar to those observed with the monoclonal antibody generated against BCRP [31]. This result was confirmed and extended by the plasma membrane staining observed by confocal microscopy in MCF-7 AdVp3000 cells with antibodies raised to peptides from different regions of ABCG2. New results from immuno-electron microscopy, which are the first of their kind, support these findings. Further, by immunohistochemistry, both the 391 and the 405 antibodies stain the plasma membrane in the chorionic villi of the placenta. However, the decidual cells within the placenta demonstrate cytoplasmic staining. One possible interpretation of this result is that the localization may vary, depending upon the cell type, the level of expression, or potentially upon dimerization partners.

The question of dimerization is a second intriguing issue for ABCG2. As a half-transporter, it should dimerize to form a functional ABC protein, with two ATP binding domains and two sets of transmembrane regions. Protein database searches revealed the *Drosophila white* gene product to be the closest match. The product of the *white* gene is known to dimerize with that of the *brown* or *scarlet* gene, to transport guanine or tryptophan, precursors for the formation of eye pigment [32]. The *white* gene product does not appear to make a functional homodimer. These conclusions are based principally upon mutational analysis, and detailed structural studies of the proteins have not been made. The fact that transfection studies confirm the ability of ABCG2 to confer a resistant phenotype suggests that homodimers are in this case functional [22,33]. Studies with ABCG2 in non-reducing conditions, and following chemical cross-linking, as well as immunoprecipitation experiments, suggest that dimerization, and possibly higher orders of oligomerization, may occur. However, the formation of non-specific protein complexes in the presence of chemical cross-linkers and under non-denaturating conditions, cannot be excluded. Kage et al. [34] also reported a high-molecular-weight band detectable by ABCG2 antibodies under non-reducing conditions and argued that the dimerization of ABCG2 is dependent upon disulfide bridges. Functional studies, for example, with cysteine-less mutants would be required to confirm this hypothesis. Data demonstrating the drug-modulatable ATPase activity of ABCG2 show that the protein is catalytically active under reducing conditions [22], which argues against the dependence on disulfide bridge formation

for ABCG2 function. The model of SUR in which four molecules together with the K_{IR} subunits join to form a functional potassium channel, suggests that the possibility of multimers should not be excluded [35]. Oligomeric forms of P-glycoprotein have also been suggested [36].

By immuno-electron microscopy, we confirmed both the plasma membrane and intracellular localization of ABCG2. Interestingly, it was not possible to demonstrate di- or oligomerization of ABCG2 with protein A gold labeling as only separate grains were observed. This, however, does not exclude dimerization, and could be due to technical difficulties, as the relatively large gold particles may have prevented close approximation of a second large particle on the dimer.

In summary, we have identified three polyclonal antibodies derived from ABCG2 peptides, one 5′ to Walker A, one including Walker B, and the third between the two, near the C signature region characteristic of ABC transporters. All three recognize ABCG2 on immunoblot analysis, and by immunohistochemical analysis. A fourth antibody made to recognize a putative extracellular domain failed to hybridize to ABCG2 on immunoblot, or by immunohistochemistry. Further studies are needed to determine whether other dimerization partners for ABCG2 can be found. High levels of expression on the plasma membrane of synchitiotrophoblastic cells of the chorionic villi of the placenta suggest a role for protection of the developing fetus from xenobiotics. Numerous questions regarding the role of ABCG2 in normal physiology and in clinical oncology remain. Recently, it has been reported to be responsible for the "side-population" phenotype of human stem cells [37]. The early identification of inhibitors suggests the feasibility of drug resistance reversal studies, and guarded optimism for improved chemotherapeutic efficacy.

Acknowledgements

We wish to thank Susanne Sørensen and Lena Rasmussen for excellent technical assistance. T.L. is supported by The Danish Cancer association, grant no. 99 100 31, The Novo Nordisk Foundation, Fru Astrid Thaysens Legat for Lægevidenskabelig Grundforskning, and A.P. Møller Fonden til Lægevidenskabens Fremme.

References

[1] K. Miyake, L.A. Mickley, T. Litman, L. Greenberger, Z. Zhan, R. Robey, B. Christensen, M. Brangi, M. Dean, A.T. Fojo, S.E. Bates, Cancer Res. 59 (1999) 8.
[2] L.A. Doyle, W. Yang, L.E. Abruzzo, T. Krogmann, Y. Gao, A.K. Rishi, D.D. Ross, Proc. Natl. Acad. Sci. U. S. A. 95 (1998) 15665.
[3] R. Allikmets, L.M. Schrim, A. Hutchinson, V. Romano-Spica, M. Dean, Cancer Res. 58 (1998) 5337.
[4] T. Litman, M. Brangi, E. Hudson, P. Fetsch, A. Abati, D.D. Ross, K. Miyake, J.H. Resau, S.E. Bates, J. Cell Sci. 113 (2000) 2011.
[5] M. Brangi, T. Litman, A. Nishiyama, K. Nishiyama, G. Kohlhagen, C. Takimoto, R. Robey, Y. Pommier, A.T. Fojo, S.E. Bates, Cancer Res. 59 (1999) 5938.
[6] I. Klein, B. Sarkadi, A. Varadi, Biochim. Biophys. Acta 1461 (1999) 236.
[7] J.D. Allen, R.F. Brinkhuis, J. Wijnholds, A.H. Schinkel, Cancer Res. 59 (2000) 4237.
[8] Y. Honjo, C.A. Hrycyna, W.Y. Medina-Perez, R.W. Robey, A. van de Laar, T. Litman, M. Dean, S.E. Bates, Cancer Res. 61 (2001) 6635.
[9] C.F. Higgins, Cell 82 (1995) 693.
[10] M. Dean, Y. Hamon, G. Chimini, J. Lipid Res. 42 (2001) 1007.
[11] Y. Wang, D.S. Guttoh, M.J. Androlewicz, Methods Enzymol. 292 (1998) 745.
[12] A. Townsend, J. Trowsdale, Semin. Cell Biol. 4 (1993) 53.
[13] F. Kok, S. Neumann, C.-O. Sarde, S. Zheng, K.-H. Wu, H.-M. Wei, J. Bergin, P.A. Watkins, S. Gould, G. Sack, H. Moser, J.-L. Mandel, K.D. Smith, Human Mutat. 6 (1995) 104.
[14] D.L. Hogue, L. Liu, V. Ling, J. Mol. Biol. 285 (1999) 379.
[15] R. Allikmets, A. Hutchinson, N.D. Schueck, M. Dean, D.M. Koeller, Hum. Mol. Genet. 8 (1999) 743.
[16] S.K. Rabindran, H. He, M. Singh, E. Brown, K.I. Collins, T. Annable, L. Greenberger, Cancer Res. 58 (1998) 5850.
[17] J.S. Lee, S. Scala, Y. Matsumoto, R. Robey, Z. Zhan, B. Dickstein, G. Altenberg, S.E. Bates, J. Cell. Biochem. 65 (1997) 1.
[18] R.W. Robey, W.Y. Medina Pérez, K. Nishiyama, T. Lahusen, K. Miyake, T. Litman, A.M. Senderowicz, D.D. Ross, S.E. Bates, Clin. Cancer Res. 7 (2001) 145.
[19] C.-H.J. Yang, J.K. Horton, K.H. Cowan, E. Schneider, Cancer Res. 55 (1995) 4004.
[20] W.C. Chan, P.D. White, Fmoc Solid-Phase Peptide Synthesis, Oxford Univ. Press, Oxford, 1999.
[21] N. Behrendt, E. Rønne, K. Danø, FEBS Lett. 336 (1993) 394.
[22] C. Ozvegy, T. Litman, G. Szakács, Z. Nagy, S. Bates, A. Varadi, B. Sarkadi, Biochem. Biophys. Res. Commun. 285 (2001) 111.
[23] U.K. Laemmli, Nature 227 (1970) 680.
[24] K.T. Tokuyasu, Histochem. J. 21 (1989) 163.
[25] K.T. Tokuyasu, J. Ultrastruct. Res. 63 (1978) 287.
[26] S.F. Altschul, T.L. Madden, A.A. Schaffer, J. Zhang, W. Miller, D.J. Lipman, Nucleic Acids Res. 25 (1997) 3389.
[27] E. Rocchi, A. Khodjakov, E.L. Volk, C.-H. Yang, T. Litman, S.E. Bates, E. Schneider, Biochem. Biophys. Res. Commun. 271 (2000) 42.
[28] J.H. Schellens, M. Maliepaard, R.J. Scheper, G. Scheffer, J.W. Jonker, J.W. Smit, J.H. Beijnen, A.H. Schinkel, Ann. N.Y. Acad. Sci. 922 (2000) 188.
[29] T. Litman, T. Druley, W.D. Stein, S.E. Bates, Cell. Mol. Life Sci. 58 (2001) 931.
[30] N. Shani, D. Valle, Methods Enzymol. 292 (1998) 753.
[31] G.L. Scheffer, M. Maliepaard, A.C.L.M. Pijnenborg, M.A. van Gastelen, M.C. de Jong, A.B. Schroeijers, D.M. van der Kolk, J.D. Allen, D.D. Ross, P. van der Valk, W.S. Dalton, J.H.M. Schellens, R.J. Scheper, Cancer Res. 60 (2000) 2589.
[32] G.D. Ewart, A.J. Howells, Methods Enzymol. 292 (1998) 213.
[33] S.K. Rabindran, D.D. Ross, L.A. Doyle, W. Yang, L.M. Greenberger, Cancer Res. 60 (2000) 47.
[34] K. Kage, S. Tsukahara, T. Sugiyama, S. Asada, T. Ishikawa, T. Tsuruo, Y. Sugimoto, Int. J. Cancer 95 (2002) 626.
[35] J. Bryan, L. Aguilar-Bryan, Biochim. Biophys. Acta 1461 (1999) 285.
[36] M.S. Poruchynsky, V. Ling, Biochemistry 33 (1994) 4163.
[37] S. Zhou, J.D. Schuetz, K.D. Bunting, A.-M. Colapietro, J. Sampath, J.J. Morris, I. Lagutina, G.C. Grosveld, M. Osawa, H. Nakauchi, B.P. Sorrentino, Nat. Med. 7 (2001) 1028.